Optical switching and bistability in four-level atomic systems

Pardeep Kumar* and Shubhrangshu Dasgupta
Department of Physics, Indian Institute of Technology Ropar, Rupnagar, Punjab 140001, India
(Received 24 February 2016; published 30 August 2016)

We explore the coherent control of nonlinear absorption of intense laser fields in four-level atomic systems. For instance, in a four-level ladder system, a coupling field creates electromagnetically induced transparency (EIT) with an Aulter-Townes doublet for the probe field while the control field is absent. A large absorption peak appears at resonance as the control field is switched on. We show how such a large absorption leads to optical switching. Further, this large absorption diminishes and a transparency window appears due to the saturation effects as the strength of the probe field is increased. We further demonstrate that the threshold of the optical bistability can be modified by suitable choices of the coupling and the control fields. In a four-level Y-type configuration, the effect of the control field on saturable absorption (SA) and reverse saturable absorption (RSA) is highlighted in the context of nonlinear absorption of the probe field. We achieve RSA and SA in a simple atomic system just by applying a control field.

DOI: 10.1103/PhysRevA.94.023851

I. INTRODUCTION

Since the invention of the laser, quantum coherence has played a vital role in controlling the nonlinear optical properties of an atomic medium [1,2]. The linear optical effect is attributed to the linear relationship between the input and output intensities. When the incident irradiance becomes large enough, a nonlinear optical effect comes into play [3]. Quantum coherence helps in enhancing the efficiencies of nonlinear optical processes (characterized by a complex third-order susceptibility), thereby eliminating the linear absorption even at low light powers [4–8]. While the real part of the third-order susceptibility (the Kerr nonlinearity) can produce significant cross-phase modulation [9,10], the imaginary part may lead to photon switching [11,12]. Further, quantum coherence can produce coherent population oscillations and sublinewidth transmission resonances in two-level [13] as well as in multilevel systems [14]. This happens as an effect of temporal modulation of the population difference between the ground and excited states. Besides transparency, electromagnetically induced absorption (EIA) may occur due to transfer of two-photon coherence between the degenerate excited levels to the degenerate ground levels [15–17]. For observation of the EIA, the multilevel systems, especially the four-level N-type systems [18,19], are the promising candidates, because they require a control field with low power. Further, two-photon coherence in a ladder-type energy-level configuration [20–22] exhibits electromagnetically induced transparency (EIT) and two-photon absorption (TPA) for a weak probe laser, in the presence of a strong coupling laser. This TPA phenomenon in the ladder systems can be dramatically modified by quantum coherence and it can make an absorptive medium transparent to the probe field [23]. Such possibility was originally proposed by Agarwal and coworkers [24] and demonstrated in [25]. Besides TPA, a large absorption at resonance can also arise due to three-photon coherence, called three-photon electromagnetically induced absorption [26,27].

All the above nonlinear phenomena assume a probe field whose strength is such that it is enough to consider the coherence only up to a finite order of the probe field (i.e., only a finite order of susceptibility, say, up to third order). However, when the intensity of the probe field is increased, one needs to investigate the response of the medium for all orders of the probe field, which gives rise to several interesting optical effects, namely, optical bistability (OB). This refers to the possibility of two stable output fields for the same input field in an optical feedback network. The nonlinear interaction between a collection of atoms and the field mode along with the feedback inside an optical cavity leads to such a bistable behavior. Based on the response of the optical feedback, the bistable device can be used as an optoelectronic component, viz., an optical differential amplifier [28–30]. The optical bistability has been extensively studied in two-level [31–33] as well as in multilevel systems [34–36] due to its application in ultrafast all-optical switches [37]. Harshawardhan and Agarwal [34] have proposed that by using quantum interference induced by control fields, one can decrease the threshold of bistability. This suggests that the nonlinear effect becomes dominant even at a low input intensity.

We further investigate the role of coherence into other nonlinear optical phenomena, namely, saturable absorption (SA) and reverse saturable absorption (RSA) [38]. The SA corresponds to the decrease of the ground-state absorption of light as the input intensity increases. On the contrary, the RSA is associated with the excited-state absorption and as a consequence, the absorption inside the medium increases with the intensity of the input field. The RSA has been demonstrated in various compounds [39–43] and has found application in *optical limiting*, viz., protection of electro-optical sensors or human eyes from intense laser pulses [44].

In this paper, we explore the effect of a control field on the nonlinear absorption characteristics of a probe field in four-level atomic systems. We consider all orders of the probe field in our analysis. The effect of atomic coherence as a function of all the fields is investigated. We show that while in the absence of the control field, the system exhibits transparency for the probe field, the nonlinear excitation is enhanced as the control field is introduced in the uppermost transition of a four-level

*pradeep.kumar@iitrpr.ac.in

ladder system. This enhancement of the nonlinear absorption leads to the absorptive optical switching [11,12] in which probe absorption can be switched on and off by a control field. We present numerical results to describe the optical switching in terms of a Gaussian intensity profile of the probe field. We also describe the absorption characteristics of the atomic medium in a unidirectional ring cavity, leading to optical bistability. In our model, the threshold of the OB can be controlled by both the control and the coupling field. Further, by coupling the first excited state with a metastable state by a control field (so as to form a Y-type configuration), we show how the SA and RSA can be coherently manipulated when both the coupling field and the probe field are of the same polarization and the same intensity. Note that here we demonstrate the RSA effect in a simple *atomic system* thanks to the coherent *control field*.

The structure of the paper is as follows. In Sec. II, we discuss the four-level ladder model configuration along with its relevant equations. In Sec. III, we describe how nonlinear absorption and optical bistability can be coherently controlled in such a system. Further, in Sec. IV, the SA and RSA effects are highlighted in a four-level Y-type system. We conclude the paper in Sec. V.

II. MODEL

To explore the nonlinear absorption characteristics of the probe field and optical bistability, we consider a four-level ladder scheme [45], as shown in Fig. 1, that comprises a ground state $|1\rangle$ and three excited states $|2\rangle$, $|3\rangle$, and $|4\rangle$, in increasing order of frequency. The coupling field $\vec{E}_1 = \hat{\pi}\varepsilon_1 e^{-i\omega_{G_1}t} +$ c.c. (the probe field $\vec{E}_2 = \hat{\sigma}_+\varepsilon_2 e^{-i\omega_{G_2}t} +$ c.c.) with a Rabi frequency $2G_1 = \frac{2\vec{d}_{21}\cdot\hat{\pi}\varepsilon_1}{\hbar}$ ($2G_2 = \frac{2\vec{d}_{32}\cdot\hat{\sigma}_+\varepsilon_2}{\hbar}$) drives the $|1\rangle \leftrightarrow |2\rangle$ ($|2\rangle \leftrightarrow |3\rangle$) transition, where $\varepsilon_i (i = 1,2)$ represents the amplitude of the field and $\vec{d}_{ij}$ is the electric dipole moment matrix element between the levels $|i\rangle$ and $|j\rangle$. Here, ω_{G_1} (ω_{G_2}) denotes the frequency of the coupling (probe) field.

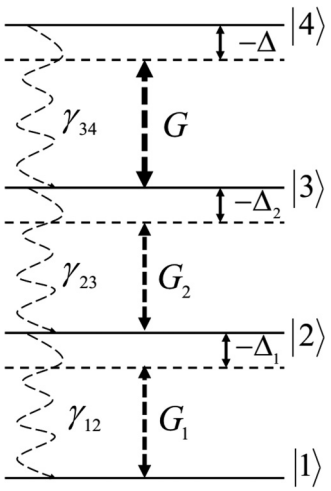

FIG. 1. Schematic of energy-level structure of a four-level ladder system. The coupling field of Rabi frequency $2G_1$ and the control field of Rabi frequency $2G$ induce the transitions $|1\rangle \leftrightarrow |2\rangle$ and $|3\rangle \leftrightarrow |4\rangle$, respectively, while a probe field of Rabi frequency $2G_2$ interacts with $|2\rangle \leftrightarrow |3\rangle$.

We apply a control field $\vec{E}_c = \hat{\sigma}_-\varepsilon_c e^{-i\omega_c t} +$ c.c. of frequency ω_c and amplitude ε_c on the transition $|3\rangle \leftrightarrow |4\rangle$. Let $2G = 2(\frac{\vec{d}_{43}\cdot\hat{\sigma}_-\varepsilon_c}{\hbar})$ be the Rabi frequency of the control field $\vec{E}_c$. The transitions $|1\rangle \leftrightarrow |3\rangle$, $|2\rangle \leftrightarrow |4\rangle$, and $|1\rangle \leftrightarrow |4\rangle$ are electric dipole forbidden.

The Hamiltonian for the system under consideration in the dipole approximation can be written as

$$\begin{aligned}\hat{H} = \hbar[&\omega_{21}|2\rangle\langle 2| + \omega_{31}|3\rangle\langle 3| + \omega_{41}|4\rangle\langle 4|]\\ &- [(\vec{d_{21}}|2\rangle\langle 1| + \text{H.c.})\cdot\vec{E}_1]\\ &- [(\vec{d_{32}}|3\rangle\langle 2| + \text{H.c.})\cdot\vec{E}_2]\\ &- [(\vec{d_{43}}|4\rangle\langle 3| + \text{H.c.})\cdot\vec{E}_c]. \end{aligned} \quad (1)$$

Here $\hbar\omega_{\alpha\beta}$ is the energy difference between the levels $|\alpha\rangle$ and $|\beta\rangle$ and zero of energy is defined at the level $|1\rangle$. The dynamical evolution of the system can be described by a Markovian master equation, and the relevant density matrix equations obtained for the four-level ladder system are given in the Appendix [see Eqs. (A1)]. Note that Eqs. (A1) consider the mutual effect of atomic coherence and all the relevant fields.

The induced polarization at a frequency ω_{G_2} on the transition $|2\rangle \leftrightarrow |3\rangle$ will be obtained from the off-diagonal matrix element $\tilde{\rho}_{32}$:

$$P(\omega_{G_2}) = \mathcal{N}\vec{d}_{23}\tilde{\rho}_{32}\ , \quad (2)$$

where, $\mathcal{N}$ is the number density of the medium. Below, we study the propagation of the field through the medium using Maxwell's equations. Using the slowly varying envelope approximation, the equations for field propagation can be expressed as

$$\begin{aligned}\left(\frac{\partial}{\partial z} + \frac{1}{c}\frac{\partial}{\partial t}\right)G_1 &= i\eta_{12}\tilde{\rho}_{21}, \quad \eta_{12} = 3\lambda_{12}^2\mathcal{N}\gamma_{12}/4\pi,\\ \left(\frac{\partial}{\partial z} + \frac{1}{c}\frac{\partial}{\partial t}\right)G_2 &= i\eta_{23}\tilde{\rho}_{32}, \quad \eta_{23} = 3\lambda_{23}^2\mathcal{N}\gamma_{23}/4\pi,\\ \left(\frac{\partial}{\partial z} + \frac{1}{c}\frac{\partial}{\partial t}\right)G &= i\eta_{34}\tilde{\rho}_{43}, \quad \eta_{34} = 3\lambda_{34}^2\mathcal{N}\gamma_{34}/4\pi, \end{aligned} \quad (3)$$

where η_{ij} and λ_{ij} are the coupling constant and wavelength for the $|i\rangle \leftrightarrow |j\rangle$ transition, respectively.

III. RESULTS

For the numerical studies, we consider relevant transitions in ^{23}Na atoms [46], where $|1\rangle = 3S_{1/2}$, $|2\rangle = 3P_{1/2}$, $|3\rangle = 3D_{3/2}$, and $|4\rangle = 8P_{1/2}$. The respective transition wavelengths and decay rates are $\lambda_{12} = 594$ nm and $\gamma_{12} \approx 9$ MHz (for $|1\rangle \leftrightarrow |2\rangle$ transition), $\lambda_{23} = 821$ nm and $\gamma_{23} \approx 6$ MHz (for $|2\rangle \leftrightarrow |3\rangle$ transition), $\lambda_{34} = 986$ nm and $\gamma_{34} \approx 0.005$ MHz (for $|3\rangle \leftrightarrow |4\rangle$ transition). Further, for numerical results, we set $\gamma_{12} \approx \gamma_{23} \approx \gamma$, unless stated otherwise.

A. Control of transmission

To describe the transmission of the field $\vec{E}_2$, the field equations [Eq. (3)] are solved in the steady-state limit, i.e., $(\partial G_i/\partial t) = (\partial\tilde{\rho}_{ij}/\partial t) = 0$. We do not make any approximation of the strength of the fields, so we resort to solving the set of simultaneous coupled equations numerically to all orders

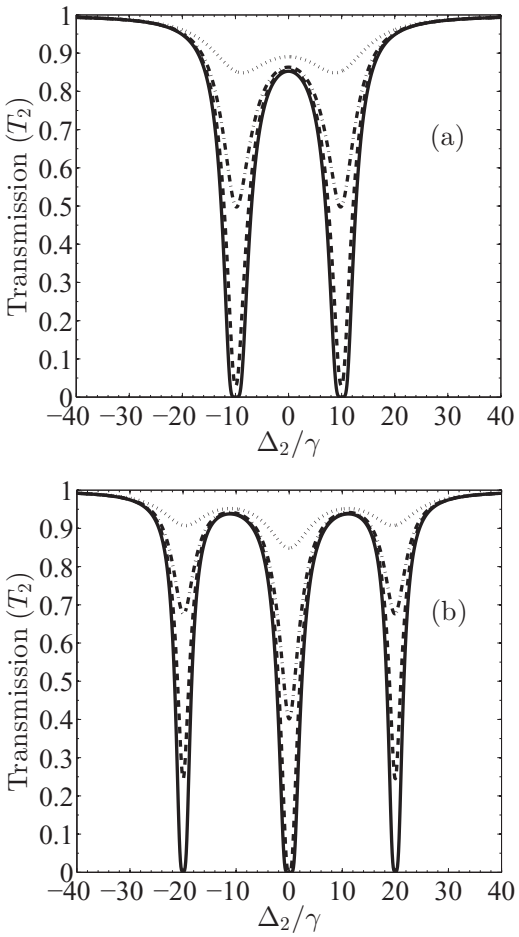

FIG. 2. Variation of transmission (T_2) with detuning (Δ_2/γ) for (a) $G_1 = 10\gamma$, $G = 0$ and (b) $G_1 = 10\gamma$, $G = 10\gamma$. The common parameters of the above graphs are $G_2 = \gamma$ (solid line), $G_2 = 3\gamma$ (dashed line), $G_2 = 5\gamma$ (dot-dashed line), and $G_2 = 10\gamma$ (dotted line), $\Delta_1 = 0$, $\Delta = 0$, $\mathcal{N} = 10^{10}$ cm^{-3}, $\eta_{12} = 12$, $\eta_{23} = 16$, $\eta_{34} = 0.2$, and $\gamma_{\text{coll}} = 0$.

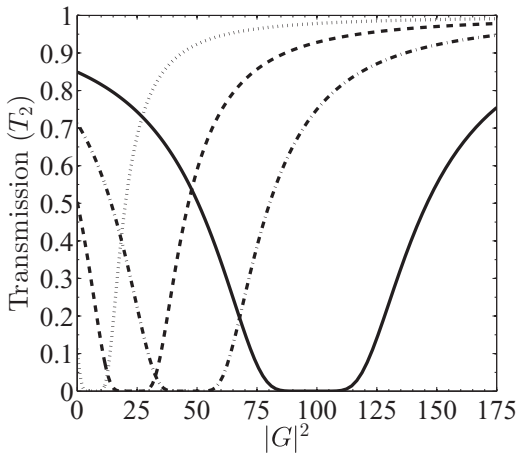

FIG. 3. Variation of transmission (T_2) with intensity of control field ($|G|^2$) for $G_1 = 3\gamma$ (dotted line), $G_1 = 5\gamma$ (dashed line), $G_1 = 7\gamma$ (dot-dashed line), and $G_1 = 10\gamma$ (solid line). Here, we have chosen $G_2 = 0.01\gamma$ and $\Delta_2 = 0$ and the other parameters are the same as in Fig. 2.

of these fields. To obtain the polarization, we solve Eqs. (A1) (in Appendix) in steady state and then integrate Eq. (3) over the length of the medium. The absorption spectrum of the probe field is shown in Fig. 2. In the absence of the control field ($G = 0$), clearly, a transparency window appears around the resonance [Fig. 2(a)] that pertains to EIT in a three-level system in ladder configuration. For a lower strength of the field $\vec{E}_2$ (viz., $G_2 = \gamma$), the Aulter-Townes absorption doublet also arises at $\Delta_2 = \pm G_1$, which can be attributed to single-photon absorption from dressed states $|\pm\rangle_{12}$ to $|3\rangle$, where $|\pm\rangle_{12} = \frac{1}{\sqrt{2}}(|1\rangle \pm |2\rangle)$ are the partial dressed states created by the resonant coupling field. The destructive interference between the transitions $|3\rangle \leftrightarrow |+\rangle_{12}$ and $|3\rangle \leftrightarrow |-\rangle_{12}$ gives rise to this transparency at resonance. (Note that this transparency window does not correspond to zero absorption, due to the decay channel $|3\rangle \rightarrow |2\rangle$).

For *larger* values of G_2, the transparency becomes prominent at resonance as the coherent absorption dominates the decay of the level $|3\rangle$. It is to be emphasized that the increase in transparency with the increase of the probe field is a consequence of the incoherent population distribution among various levels at the steady state.

When the control field is introduced on the $|3\rangle \leftrightarrow |4\rangle$ transition (viz. $G = G_1$), the system becomes highly absorptive. While the new absorption peak appears at resonance [at $\Delta_2 = \pm(G - G_1)$] for smaller values of $G_2 = \gamma$ [Fig. 2(b)], the control field also shifts the absorption doublet to $\Delta_2 = \pm(G + G_1)$. These absorption characteristics can be understood in terms of different partial dressed states [47]. The highest central absorption peak at $\Delta_2 = \pm(G - G_1)$, i.e., at resonance, arises due to the quantum interference between the transitions $|+\rangle_{34} \leftrightarrow |+\rangle_{12}$ and $|-\rangle_{34} \leftrightarrow |-\rangle_{12}$, where $|\pm\rangle_{34} = \frac{1}{\sqrt{2}}(|3\rangle \pm |4\rangle)$ are the dressed states produced by the control field G. On the other hand, the lower absorption peaks at $\Delta_2 = \pm(G + G_1)$ are the consequences of the transitions $|+\rangle_{34} \leftrightarrow |-\rangle_{12}$ and $|-\rangle_{34} \leftrightarrow |+\rangle_{12}$, respectively. For larger values of G_2, the resonant absorption in the $|2\rangle \rightarrow |3\rangle$ transition becomes less again due to the incoherent population distribution (leading to saturation).

As discussed above, for $G = G_1$ and smaller values of G_2, the probe field G_2 gets fully absorbed at resonance. In support of this, we display in Fig. 3 the transmission of the resonant probe field as a function of the intensity of the control field. It immediately becomes obvious that transmission vanishes at $G = G_1$. For $G < G_1$ the absorption dominates with an increase in the control-field intensity, while in the region $G > G_1$, the transmission increases with increase of the control field. Thus, the condition $G = G_1$ is suitable to produce nonlinear absorptive switching because the probe absorption can be turned on and off by the control field. It should be borne in mind that such a large absorption at resonance for a weaker probe field occurs due to quantum-interference-enhanced nonlinear absorption with the inhibition of linear absorption.

We now demonstrate the above analysis in terms of the absorptive photon switching with reference to a Gaussian

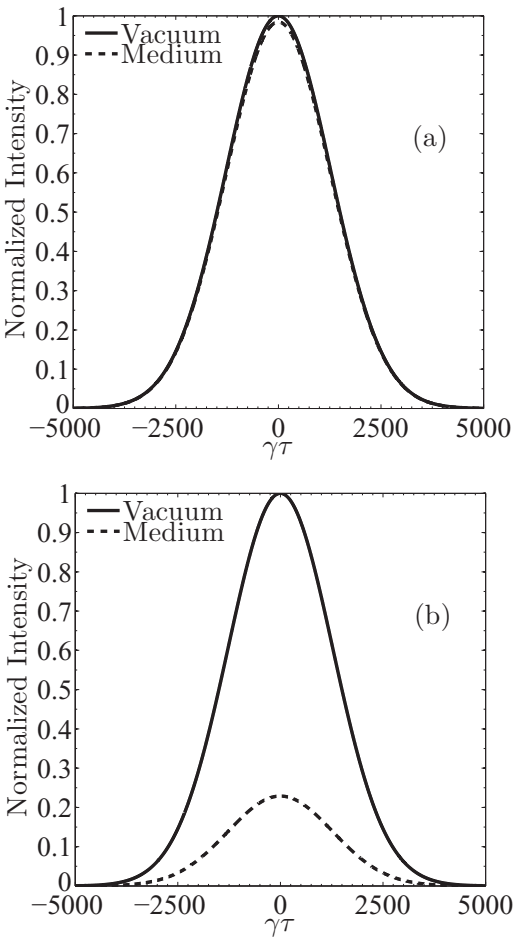

FIG. 4. Time dependence of the normalized Gaussian pulse after traveling through vacuum (solid line) and the atomic medium (dashed line) of length $L = 1$ cm for (a) $G = 0$ and (b) $G = 10\gamma$. The parameters chosen are $G_1 = 10\gamma$, $G_2 = 0.1\gamma$, $\sigma = 2\pi \times 5$ kHz, and $\tau = t - L/c$; other parameters are the same as in Fig. 2.

probe pulse with a normalized envelope given by [48]

$$\varepsilon(\omega) = \varepsilon_0 \frac{1}{\sigma\sqrt{\pi}} \exp(-\omega^2/\sigma^2),$$
$$\varepsilon(t) = \varepsilon_0 \frac{1}{\sqrt{2\pi}} \exp\left(-\sigma_t^2 t^2/4\right), \tag{4}$$

where $\sigma(\sigma_t = 2/\sigma)$ denotes the width of the pulse in the frequency (time) domain and ε_0 is the pulse amplitude. For numerical calculation, we choose $\sigma = 2\pi \times 5$ kHz ($\sigma_t = 64\ \mu$s). In Fig. 4, we display the effect of the control field on the absorption of a Gaussian-shaped probe pulse, Eq. (4). In the absence of the control field, the output pulse remains equally intense as that of the input pulse thanks to the EIT created by the coupling field of Rabi frequency $G_1 = 10\gamma$ as shown in Fig. 4(a). However, a significant decrease in the output intensity occurs in the presence of the control field of Rabi frequency $G = G_1$ as depicted in Fig. 4(b). Thus, the probe pulse can be turned on and off by the control field which demonstrates realization of the nonlinear absorptive photon switching [11,12].

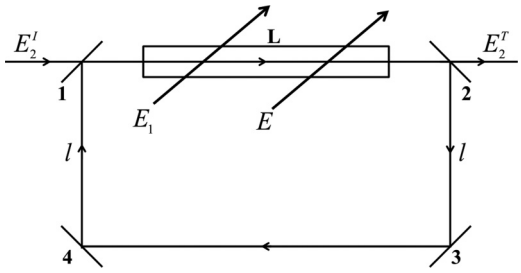

FIG. 5. Unidirectional ring cavity with mirrors 3 and 4 as perfect reflectors, while mirrors 1 and 2 obey $R + T = 1$. The atomic medium of length L is inserted in the cavity. E_2^I and E_2^T are the incident and transmitted fields and $\vec{E}$ and $\vec{E}_1$ are the control and coupling fields, respectively.

B. Control of optical bistability

Now, we consider an optical feedback scenario, in which, an ensemble of $\mathcal{N}$ atoms in four-level ladder configuration (Fig. 1) is placed in a unidirectional cavity of total length L_T as depicted in Fig. 5. Here, mirrors 3 and 4 are perfect reflectors, while R and T $(=1 - R)$ are the reflection and transmission coefficients of the semi-silvered mirrors 1 and 2. The total electric field experienced by the atoms placed in the cavity can be written as

$$\vec{E} = \vec{\varepsilon}_1 e^{-i\omega_{G_1} t} + \vec{\varepsilon}_2 e^{-i\omega_{G_2} t} + \vec{\varepsilon}_c e^{-i\omega_G t} + \text{c.c.} \tag{5}$$

The coherent field E_2^I enters the cavity through the semi-silvered mirror 1 and induces polarization [Eq. (2)] in the medium. This field comes out of the cavity and gets partially transmitted from mirror 2 as E_2^T. Fields $\vec{E}_1$ and $\vec{E}$ do not circulate in the cavity; but these fields control the induced polarization. For a perfectly tuned cavity, the boundary conditions between the incident field E_2^I and the transmitted field E_2^T are given by [49,50]

$$E_2^T(t) = \sqrt{T} E_2(L,t),$$
$$E_2(0,t) = \sqrt{T} E_2^I(t) + R \exp(-i\delta_0) E_2(L, t - \Delta t), \tag{6}$$

where $E_2(0,t)$ is the field at the start of the sample, $E_2(L,t)$ is the field after traversing the sample of length L, $\Delta t = (2l + L)/c$ is the time taken to travel from mirror 2 to mirror 1, $\delta_0 = (\omega_c - \omega_0) L_T/c$ is the detuning with the cavity with frequency ω_c, and $L_T = 2(l + L)$ is the total length of the cavity. In the steady state, the above boundary conditions reduce to

$$E_2^T = \sqrt{T} E_2(L),$$
$$E_2(0) = \sqrt{T} E_2^I + R \exp(-i\delta_0) E_2(L). \tag{7}$$

We define a cooperation parameter $C = \alpha L/2T$ [29,30], where $\alpha = \frac{4\pi \mathcal{N} \omega_{G_2} |\vec{d}_{32}|^2}{\hbar \gamma_{32} c}$ is the absorption coefficient on the transition $|2\rangle \leftrightarrow |3\rangle$.

Figure 6(a) shows the dependence of the optical bistability on the input laser intensity G_2 in the absence of the control field ($G = 0$) for different values of G_1 without mean-field approximation [34]. In absence of the control field, the system acts as a three-level ladder system, in which the increase of G_1 leads to transparency of G_2, analogous to EIT. As seen

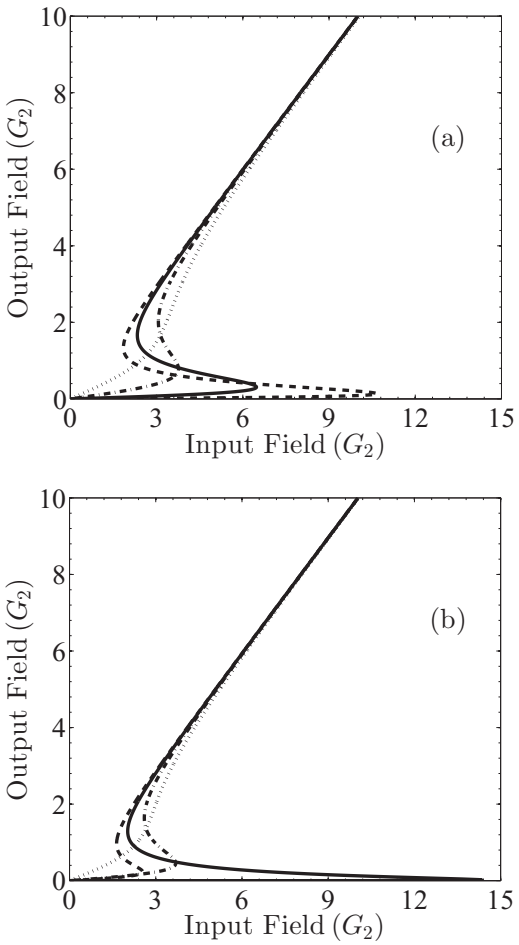

FIG. 6. Variation of output fields with input fields for (a) $G = 0$ and (b) $G = 5\gamma$. The common parameters for these graphs are $G_1 = 3\gamma$ (dashed line), $G_1 = 5\gamma$ (solid line), $G_1 = 10\gamma$ (dot-dashed line), and $G_1 = 20\gamma$ (dotted line). The parameters are chosen as $\Delta_2 = 0$ and $C = 400$; the other parameters are the same as in Fig. 2.

in Fig. 6(a), the threshold of the optical bistability decreases with increase of the input field G_1. For much larger values of $G_1 = 20\gamma$, the system actually shows the features of an optical transistor.

When the control field is *switched on*, absorption dominates at resonance for $G = G_1$. Despite this, the region for $G \lesseqgtr G_1$ corresponds to transparency. As depicted in Fig. 6(b), $G = G_1$ leads to significant increase of the threshold. On the other hand, for $G \neq G_1$, the threshold for bistability remains quite small. Thus, by working in the region $G \lesseqgtr G_1$, the nonlinearity of the atomic medium can be greatly enhanced and hence it is easier to achieve saturation for the cavity field than in the case when the control field is not applied. In fact, in the absence of the control field, one needs to apply a very large coupling field to achieve a smaller threshold [see Fig. 6(a)].

IV. CONTROL OF RSA AND SA: EFFECT OF DECAY RATES

Next, to model the SA and RSA effects, we couple the first excited state of the three-level ladder system with a metastable state by a control field, so as to form a Y-type system as shown

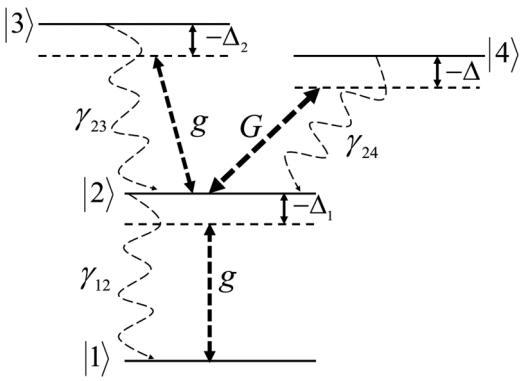

FIG. 7. Level scheme for the SA and RSA effects. The two dipole allowed transitions $|1\rangle \leftrightarrow |2\rangle$ and $|2\rangle \leftrightarrow |3\rangle$ are coupled to the fields having the same polarization and Rabi frequency $2g$. The control field drives the transition $|2\rangle \leftrightarrow |4\rangle$.

in Fig. 7. For the purpose of SA and RSA effects, we choose the fields $\vec{E}_1$ and $\vec{E}_2$ to be of the same polarization and of equal Rabi frequency $2g$. From now on we call this field a *probe field* which is interacting with transitions $|1\rangle \leftrightarrow |2\rangle$ and $|2\rangle \leftrightarrow |3\rangle$. Here, the control field of Rabi frequency $2G$ is coupled to transition $|2\rangle \leftrightarrow |4\rangle$. The relevant density matrix equations for Y-type system which describe the dynamical evolution of the system by using a Markovian master equation are given in Appendix B [see Eqs. (B1)].

Thus, the polarization induced in the medium can be written as

$$P(\omega) = \mathcal{N}\vec{d}(\tilde{\rho}_{21} + \tilde{\rho}_{32}), \tag{8}$$

where we have assumed that $\vec{d} = \vec{d}_{12} = \vec{d}_{23}$. Further, Maxwell's equations in a slowly varying envelope approximation can be written as

$$\left(\frac{\partial}{\partial z} + \frac{1}{c}\frac{\partial}{\partial t}\right)g = i(\eta_{12}\tilde{\rho}_{21} + \eta_{23}\tilde{\rho}_{32}),$$
$$\left(\frac{\partial}{\partial z} + \frac{1}{c}\frac{\partial}{\partial t}\right)G = i\eta_{24}\tilde{\rho}_{43}, \tag{9}$$

where η_{ij} represents the coupling constant for the $|i\rangle \leftrightarrow |j\rangle$ transition. To obtain transmission at the output of the medium, we integrate Eq. (9) over the length of the medium in steady state.

We first consider that level $|3\rangle$ has a decay rate larger than level $|2\rangle$. We show in Fig. 8(a) how the net transmission of the input field varies as a function of the input intensity. We find that as the input intensity increases up to a certain threshold, the system remains absorptive, in absence of the control field. This is because level $|3\rangle$ decays much faster. At a certain input threshold, when the input intensity dominates over this decay rate, the system undergoes saturation and exhibits more transmission with larger input intensity, as in the case of SA. Next when a control field is introduced, we find that the system becomes transparent for weak probe field, due to the EIT-like effect. This phenomenon can be understood as a manifestation of the partial dressed states that are comprised of levels $|2\rangle$ and $|4\rangle$. As the input intensity is increased until the input threshold, the system exhibits more absorption, leading to the RSA effect.

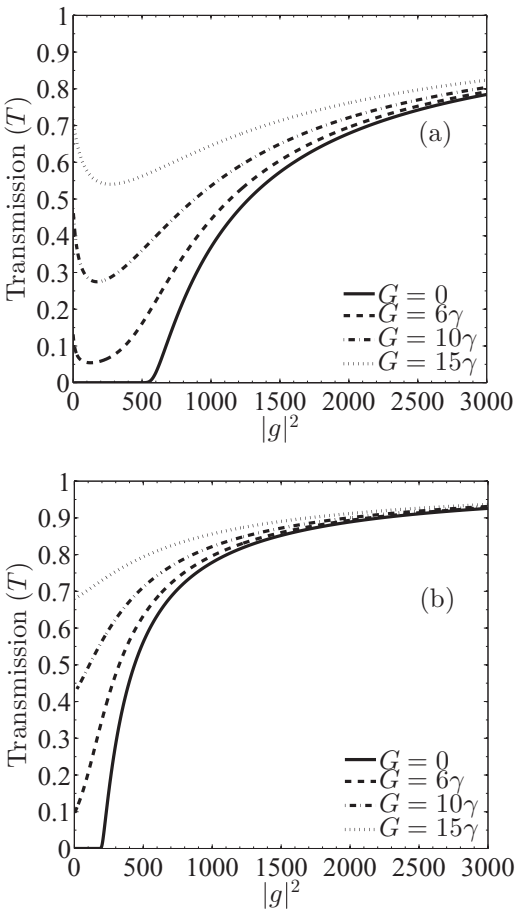

FIG. 8. Variation of transmission (T) with the intensity of the probe field for (a) $\gamma_{12}/2\pi = 5$ MHz, $\gamma_{23}/2\pi = 11$ MHz, $\gamma_{24}/2\pi = 0.97$ MHz, $\eta_{12} = 88$, $\eta_{23} = 1.5$, and $\eta_{24} = 8.8$; (b) $\gamma_{12}/2\pi = 6$ MHz, $\gamma_{23}/2\pi = 0.97$ MHz, $\gamma_{24}/2\pi = 1.1$ MHz, $\eta_{12} = 87$, $\eta_{23} = 14$, and $\eta_{24} = 10$. Here the fields are resonant, i.e., $\Delta_1 = 0$, $\Delta_2 = 0$, and $\Delta = 0$, and we have chosen $\gamma = 1$ MHz.

This is because the control field assists in further absorption by Rabi cycling the population in the $(|2\rangle, |4\rangle)$ manifold. *Clearly, just by applying a control field, one can achieve the RSA effect in a system that exhibits SA otherwise*. We illustrate the RSA effect by considering the example of the relevant energy levels of ^{85}Rb as $|1\rangle = 5S_{1/2}$, $|2\rangle = 5P_{1/2}$, $|3\rangle = 7S_{1/2}$, and $|4\rangle = 5D_{3/2}$. The respective transition wavelengths and decay rates are [51,52] $\lambda_{12} = 795$ nm and $\gamma_{12} = 2\pi \times 5$ MHz (for $|1\rangle \leftrightarrow |2\rangle$ transition), $\lambda_{23} = 762$ nm and $\gamma_{23} = 2\pi \times 11$ MHz (for $|2\rangle \leftrightarrow |3\rangle$ transition), $\lambda_{24} = 741$ nm and $\gamma_{24} = 2\pi \times 0.67$ MHz (for $|2\rangle \leftrightarrow |4\rangle$ transition). For the RSA effect, the $\hat{\pi}$-polarized field is interacting with $|1\rangle \leftrightarrow |2\rangle$ and $|2\rangle \leftrightarrow |3\rangle$ transitions, whereas the control field is $\hat{\sigma}_+$ polarized on the $|2\rangle \leftrightarrow |4\rangle$ transition.

Next we consider a situation in which level $|3\rangle$ is slowly decaying compared to the level $|2\rangle$. In this case, as the population resides in the level $|3\rangle$ for a much longer time, the system achieves saturation quickly and exhibits transparency (and SA). When a control field is introduced, this advances the saturation. This is because level $|4\rangle$ gets populated through coherent coupling to level $|2\rangle$ and thus assists in transmission. In Fig. 8(b), we display this effect of the control field on SA. For the possible realization of SA, we consider the relevant energy levels of ^{87}Rb. The designated states can be chosen as follows: $|1\rangle = 5S_{1/2}$, $|2\rangle = 5P_{3/2}$, $|3\rangle = 5D_{5/2}$, and $|4\rangle = 8S_{1/2}$. The respective transition wavelengths and decay rates are [53–55] $\lambda_{12} = 780$ nm and $\gamma_{12} = 2\pi \times 6$ MHz (for $|1\rangle \leftrightarrow |2\rangle$ transition), $\lambda_{23} = 776$ nm and $\gamma_{23} = 2\pi \times 0.97$ MHz (for $|2\rangle \leftrightarrow |3\rangle$ transition), $\lambda_{24} = 616$ nm and $\gamma_{24} = 2\pi \times 1.1$ MHz (for $|2\rangle \leftrightarrow |4\rangle$ transition). For the SA effect, a $\hat{\sigma}_+$-polarized field is interacting with $|1\rangle \leftrightarrow |2\rangle$ and $|2\rangle \leftrightarrow |3\rangle$ transitions while the polarization of the control field is $\hat{\sigma}_-$ on the $|2\rangle \leftrightarrow |4\rangle$ transition.

V. CONCLUSIONS

In conclusion, we have demonstrated the possibility of coherent control of nonlinear absorption of a probe field in four-level atomic systems. We have shown that in a four-level ladder system, the medium which otherwise is transmissive for a weaker probe field becomes absorptive as the control field is introduced. Such a large nonlinear absorption leads to the absorptive optical switching. Further, as the strength of the probe field is increased, a saturation effect gives rise to large transparency. We further have shown that the threshold for optical bistability can be manipulated by both the coupling field and the control field. Further, in a four-level Y configuration, we have discussed how the control field can work as a knob to switch from RSA to SA.

APPENDIX A: DENSITY MATRIX EQUATIONS FOR FOUR-LEVEL LADDER SYSTEM

To describe the dynamics of the four-level ladder system, we use the Markovian master equation and obtain the following density matrix equations:

$$
\begin{aligned}
\dot{\tilde{\rho}}_{22} &= \gamma_{23}\tilde{\rho}_{33} - \gamma_{12}\tilde{\rho}_{22} + i(G_1\tilde{\rho}_{12} - G_1^*\tilde{\rho}_{21}) - i(G_2\tilde{\rho}_{23} - G_2^*\tilde{\rho}_{32}),\\
\dot{\tilde{\rho}}_{33} &= \gamma_{34}\tilde{\rho}_{44} - \gamma_{23}\tilde{\rho}_{33} + i(G_2\tilde{\rho}_{23} - G_2^*\tilde{\rho}_{32}) - i(G\tilde{\rho}_{34} - G^*\tilde{\rho}_{43}),\\
\dot{\tilde{\rho}}_{44} &= -\gamma_{34}\tilde{\rho}_{44} + i(G\tilde{\rho}_{34} - G^*\tilde{\rho}_{43}),\\
\dot{\tilde{\rho}}_{21} &= (i\Delta_1 - \Gamma_{21})\tilde{\rho}_{21} + iG_1(1 - 2\tilde{\rho}_{22} - \tilde{\rho}_{33} - \tilde{\rho}_{44}) + iG_2^*\tilde{\rho}_{31},\\
\dot{\tilde{\rho}}_{32} &= (i\Delta_2 - \Gamma_{32})\tilde{\rho}_{32} + iG_2(\tilde{\rho}_{22} - \tilde{\rho}_{33}) + iG^*\tilde{\rho}_{42} - iG_1^*\tilde{\rho}_{31},\\
\dot{\tilde{\rho}}_{43} &= (i\Delta - \Gamma_{43})\tilde{\rho}_{43} + iG(\tilde{\rho}_{33} - \tilde{\rho}_{44}) - iG_2^*\tilde{\rho}_{42},\\
\dot{\tilde{\rho}}_{31} &= [i(\Delta_1 + \Delta_2) - \Gamma_{31}]\tilde{\rho}_{31} + iG^*\tilde{\rho}_{41} + iG_2\tilde{\rho}_{21} - iG_1\tilde{\rho}_{32},\\
\dot{\tilde{\rho}}_{42} &= [i(\Delta_2 + \Delta) - \Gamma_{42}]\tilde{\rho}_{42} + iG\tilde{\rho}_{32} - iG_2\tilde{\rho}_{43} - iG_1^*\tilde{\rho}_{41},\\
\dot{\tilde{\rho}}_{41} &= [i(\Delta_1 + \Delta_2 + \Delta) - \Gamma_{41}]\tilde{\rho}_{41} + iG\tilde{\rho}_{31} - iG_1\tilde{\rho}_{42},
\end{aligned}
\tag{A1}
$$

together with the condition $\sum_{i=1}^{4}\tilde{\rho}_{ii}=1$. Here, $\Delta_1=\omega_{G_1}-\omega_{21}$ ($\Delta_2=\omega_{G_2}-\omega_{32}$) is the detuning of the field $\vec{E}_1$ ($\vec{E}_2$) from the transition $|1\rangle\leftrightarrow|2\rangle$ ($|2\rangle\leftrightarrow|3\rangle$) and $\Delta=\omega_c-\omega_{43}$ is the detuning of the control field from the transition $|3\rangle\leftrightarrow|4\rangle$. The spontaneous emission rate from level $|j\rangle$ to $|i\rangle$ is represented by γ_{ij}, and $\Gamma_{ij}=\frac{1}{2}\sum_k(\gamma_{ki}+\gamma_{kj})+\gamma_{\rm coll}$ describes the dephasing rate of coherence between the levels $|j\rangle$ and $|i\rangle$, $\gamma_{\rm coll}$ being the collisional decay rate. The highly oscillating terms in Eq. (A1) are neglected with rotating-wave approximations by choosing the transformations for the density matrix elements as $\tilde{\rho}_{21}=\rho_{21}e^{i\omega_{G_1}t}$, $\tilde{\rho}_{32}=\rho_{32}e^{i\omega_{G_2}t}$, $\tilde{\rho}_{43}=\rho_{43}e^{i\omega_c t}$, $\tilde{\rho}_{31}=\rho_{31}e^{i(\omega_{G_1}+\omega_{G_2})t}$, $\tilde{\rho}_{42}=\rho_{42}e^{i(\omega_c+\omega_{G_2})t}$, $\tilde{\rho}_{41}=\rho_{41}e^{i(\omega_c+\omega_{G_1}+\omega_{G_2})t}$, and $\tilde{\rho}_{ii}=\rho_{ii}$.

APPENDIX B: DENSITY MATRIX EQUATIONS FOR Y-TYPE SYSTEM

The equations of evolution of density matrix by using the Markovian master equation for Y-type systems are as follows:

$$
\begin{aligned}
\dot{\tilde{\rho}}_{11}&=\gamma_{12}\tilde{\rho}_{22}-i(g\tilde{\rho}_{12}-g^*\tilde{\rho}_{21}),\\
\dot{\tilde{\rho}}_{22}&=-\gamma_{12}\tilde{\rho}_{22}+\gamma_{23}\tilde{\rho}_{33}+\gamma_{24}\tilde{\rho}_{44}+i(g\tilde{\rho}_{12}-g^*\tilde{\rho}_{21}),\\
&\quad -i(g\tilde{\rho}_{23}-g^*\tilde{\rho}_{32})-i(G\tilde{\rho}_{24}-G^*\tilde{\rho}_{42}),\\
\dot{\tilde{\rho}}_{33}&=-\gamma_{23}\tilde{\rho}_{33}+i(g\tilde{\rho}_{23}-g^*\tilde{\rho}_{32}),\\
\dot{\tilde{\rho}}_{44}&=-\gamma_{24}\tilde{\rho}_{44}-i(G\tilde{\rho}_{24}-G^*\tilde{\rho}_{42}),\\
\dot{\tilde{\rho}}_{21}&=(i\Delta_1-\Gamma_{21})\tilde{\rho}_{21}+ig(1-2\tilde{\rho}_{22}-\tilde{\rho}_{33}-\tilde{\rho}_{44}),\\
&\quad +ig^*\tilde{\rho}_{31}+iG^*\tilde{\rho}_{41},\\
\dot{\tilde{\rho}}_{32}&=(i\Delta_2-\Gamma_{32})\tilde{\rho}_{32}+ig(\tilde{\rho}_{22}-\tilde{\rho}_{33})-ig^*\tilde{\rho}_{31}+iG\tilde{\rho}_{34},\\
\dot{\tilde{\rho}}_{42}&=(i\Delta-\Gamma_{42})\tilde{\rho}_{42}+iG(\tilde{\rho}_{22}-\tilde{\rho}_{44})-ig^*\tilde{\rho}_{43}-ig^*\tilde{\rho}_{41},\\
\dot{\tilde{\rho}}_{31}&=[i(\Delta_1+\Delta_2)-\Gamma_{31}]\tilde{\rho}_{31}-ig\tilde{\rho}_{32}+ig\tilde{\rho}_{21},\\
\dot{\tilde{\rho}}_{43}&=[i(\Delta-\Delta_2)-\Gamma_{43}]\tilde{\rho}_{43}+iG\tilde{\rho}_{23}-ig^*\tilde{\rho}_{42},\\
\dot{\tilde{\rho}}_{41}&=[i(\Delta_1+\Delta)-\Gamma_{41}]\tilde{\rho}_{41}+iG\tilde{\rho}_{21}-ig\tilde{\rho}_{42}.
\end{aligned}
\tag{B1}
$$

Here we have used $\sum_{i=1}^{4}\tilde{\rho}_{ii}=1$. The detunings of the fields from respective transitions are given by $\Delta_1=\omega_{G_1}-\omega_{12}$, $\Delta_2=\omega_{G_2}-\omega_{23}$, and $\Delta=\omega_c-\omega_{24}$. Further, the transformations used to remove the the rapidly oscillating terms in Eqs. (B1) are $\tilde{\rho}_{21}=\rho_{21}e^{i\omega_{G_1}t}$, $\tilde{\rho}_{32}=\rho_{32}e^{i\omega_{G_2}t}$, $\tilde{\rho}_{42}=\rho_{42}e^{i\omega_c t}$, $\tilde{\rho}_{31}=\rho_{31}e^{i(\omega_{G_1}+\omega_{G_2})t}$, $\tilde{\rho}_{41}=\rho_{41}e^{i(\omega_{G_1}+\omega_c)t}$, $\tilde{\rho}_{43}=\rho_{43}e^{i(\omega_c-\omega_{G_2})t}$, and $\tilde{\rho}_{ii}=\rho_{ii}$.

[1] M. O. Scully and M. S. Zubairy, *Quantum Optics* (Cambridge University, Cambridge, 1997).

[2] Z. Ficek and S. Swain, *Quantum Interference and Coherence* (Springer, New York, 2007).

[3] R. W. Boyd, *Nonlinear Optics* (Academic, New York, 2008).

[4] S. E. Harris, J. E. Field, and A. Imamoğlu, Nonlinear Optical Processes Using Electromagnetically Induced Transparency, Phys. Rev. Lett. **64**, 1107 (1990).

[5] S. E. Harris and L. V. Hau, Nonlinear Optics at Low Light Levels, Phys. Rev. Lett. **82**, 4611 (1999).

[6] H. Wang, D. Goorskey, and M. Xiao, Enhanced Kerr Nonlinearity via Atomic Coherence in a Three-Level Atomic System, Phys. Rev. Lett. **87**, 073601 (2001).

[7] H. Kang and Y. Zhu, Observation of Large Kerr Nonlinearity at Low Light Intensities, Phys. Rev. Lett. **91**, 093601 (2003).

[8] J. Sheng, X. Yang, H. Wu, and M. Xiao, Modified self-Kerr-nonlinearity in a four-level N-type atomic system, Phys. Rev. A **84**, 053820 (2011).

[9] H. Schmidt and A. Imamoğlu, Giant Kerr nonlinearities obtained by electromagnetically induced transparency, Opt. Lett. **21**, 1936 (1996).

[10] H. Schmidt and A. Imamoğlu, High-speed properties of a phase-modulation scheme based on electromagnetically induced transparency, Opt. Lett. **23**, 1007 (1998).

[11] S. E. Harris and Y. Yamamoto, Photon Switching by Quantum Interference, Phys. Rev. Lett. **81**, 3611 (1998).

[12] M. Yan, E. G. Rickey, and Y. Zhu, Observation of absorptive photon switching by quantum interference, Phys. Rev. A **64**, 041801(R) (2001).

[13] R. W. Boyd, M. G. Raymer, P. Narum, and D. J. Harter, Four-wave parametric interactions in a strongly driven two-level system, Phys. Rev. A **24**, 411 (1981).

[14] S. Kumar, T. Lauprêtre, F. Bretenakr, F. Goldfarb, and R. Ghosh, Polarization-dependent manipulation of optical properties in a tripod system, Phys. Rev. A **88**, 023852 (2013).

[15] A. M. Akulshin, S. Barreiro, and A. Lezama, Electromagnetically induced absorption and transparency due to resonant two-field excitation of quasidegenerate levels in Rb vapor, Phys. Rev. A **57**, 2996 (1998).

[16] A. Lezama, S. Barreiro, and A. M. Akulshin, Electromagnetically induced absorption, Phys. Rev. A **59**, 4732 (1999).

[17] A. V. Taichenachev, A. M. Tumaikin, and V. I. Yudin, Electromagnetically induced absorption in a four-state system, Phys. Rev. A **61**, 011802(R) (1999).

[18] H. Kang, G. Hernandez, and Y. Zhu, Superluminal and slow light propagation in cold atoms, Phys. Rev. A **70**, 011801(R) (2004).

[19] T. Y. Abi-Salloum, B. Henry, J. P. Davis, and F. A. Narducci, Resonances and excitation pathways in four-level N-type atomic systems, Phys. Rev. A **82**, 013834 (2010).

[20] A. K. Mohapatra, T. R. Jackson, and C. S. Adams, Coherent Optical Detection of Highly Excited Rydberg States Using Electromagnetically Induced Transparency, Phys. Rev. Lett. **98**, 113003 (2007).

[21] M. Kumar and S. Singh, Electromagnetically induced transparency and slow light in three-level ladder systems: Effect of velocity-changing and dephasing collisions, Phys. Rev. A **79**, 063821 (2009).

[22] C. Liu, J. F. Chen, S. Zhang, Y.-H. Kim, M. M. T. Loy, G. K. L. Wong, and S. Du, Two-photon interferences with degenerate and nondegenerate paired photons, Phys. Rev. A **85**, 021803 (2012).

[23] W. Kaiser and C. G. B. Garrett, Two-Photon Excitation in CaF_2 : Eu^{2+}, Phys. Rev. Lett. **7**, 229 (1961).

[24] G. S. Agarwal and W. Harshawardhan, Inhibition and Enhancement of Two Photon Absorption, Phys. Rev. Lett. **77**, 1039 (1996).
[25] J.-Y. Gao, S.-H. Yang, D. Wang, X.-Z. Guo, K.-X. Chen, Y. Jiang, and B. Zhao, Electromagnetically induced inhibition of two-photon absorption in sodium vapor, Phys. Rev. A **61**, 023401 (2000).
[26] H. S. Moon and T. Jeong, Three-photon electromagnetically induced absorption in a ladder-type atomic system, Phys. Rev. A **89**, 033822 (2014).
[27] H.-R. Noh and H. S. Moon, Three-photon coherence in a ladder-type atomic system, Phys. Rev. A **92**, 013807 (2015).
[28] H. M. Gibbs, *Optical Bistability: Controlling Light with Light* (Academic, New York, 1985).
[29] E. Abraham and S. D. Smith, Optical bistability and related devices, Rep. Prog. Phys. **45**, 815 (1982).
[30] L. A. Lugiato, in *Progress in Optics*, edited by E. Wolf (North-Holland, Amsterdam, 1984), Vol. XXI, p. 69.
[31] S. L. MacCall, Instabilities in continuous-wave light propagation in absorbing media, Phys. Rev. A **9**, 1515 (1974).
[32] H. M. Gibbs, S. L. MacCall, and T. N. C. Venkatesan, Differential Gain and Bistability Using Sodium-Filled Fabry-Perot Interferometer, Phys. Rev. Lett. **36**, 1135 (1976).
[33] D. E. Grant and H. J. Kimble, Optical bistability for two-level atoms in a standing-wave cavity, Opt. Lett. **7**, 353 (1982).
[34] W. Harshawardhan and G. S. Agarwal, Controlling optical bistability using electromagnetic-field-induced transparency and quantum interferences, Phys. Rev. A **53**, 1812 (1996).
[35] A. Joshi, W. Yang, and M. Xiao, Effect of quantum interference on optical bistability in the three-level V-type atomic system, Phys. Rev. A **68**, 015806 (2003).
[36] H. A. Babu and H. Wanare, Coherent control of the refractive index using optical stability, Phys. Rev. A **87**, 033821 (2013).
[37] A. M. C. Dawes, L. Illing, S. M. Clark, and D. J. Gauthier, All optical switching in rubidium vapor, Science **308**, 672 (2005).
[38] R. L. Sutherland, *Handbook of Nonlinear Optics* (CRC, New York, 2003).
[39] L. W. Tutt and A. Kost, Optical limiting performance of C_{60} and C_{70} solutions, Nature **356**, 225 (1992).
[40] P. Chen *et al.*, Electronic Structure and Optical Limiting Behavior of Carbon Nanotubes, Phys. Rev. Lett. **82**, 2548 (1999).
[41] L. Vivien *et al.*, Single-wall carbon nanotubes for optical limiting, Chem. Phys. Lett. **307**, 317 (1999).
[42] B. Zhao, B. Cao, D. Zhou, D. Li, and W. Zhou, Nonlinear optical transmission of nanographene and its composites, J. Phys. Chem. C **114**, 12517 (2010).
[43] G.-K. Lim *et al.*, Giant broadband nonlinear optical absorption response in dispersed graphene single sheets, Nature Photon. **5**, 554 (2011).
[44] G.-J. Zhou and W.-Y. Wong, Organometallic acetylides of Pt^{II}, Au^{I} and Hg^{II} as a new generation optical power limiting materials, Chem. Soc. Rev. **40**, 2541 (2011).
[45] S. N. Sandhya, The effect of atomic coherence on absorption in four-level atomic systems: An analytical study, J. Phys. B **40**, 837 (2007).
[46] C. F. Fischer, G. Tachiev, and A. Irimia, Relativistic energy levels, lifetimes, and transition probabilities for the sodium-like to argon-like sequences, At. Data Nucl. Data Tables **92**, 607 (2006).
[47] N. Mulchan, D. G. Ducreay, R. Pina, M. Yan, and Y. Zhu, Nonlinear excitation by quantum interference in a Doppler-broadened rubidium atomic system, J. Opt. Soc. Am. B **17**, 820 (2000).
[48] P. Kumar and S. Dasgupta, Estimation of temporal separation of slow light pulses in atomic vapors by weak measurement, Phys. Rev. A **91**, 043803 (2015).
[49] R. Bonifacio and L. A. Lugiato, Cooperative effects and bistability for resonance fluorescence, Opt. Commun. **19**, 172 (1976).
[50] R. Bonifacio and L. A. Lugiato, Optical bistability and cooperative effects in resonance fluorescence, Phys. Rev. A **18**, 1129 (1978).
[51] S. Wielandy and A. L. Gaeta, Coherent Control of the Polarization of an Optical Field, Phys. Rev. Lett. **81**, 3359 (1998).
[52] R. Yu, J. Li, P. Huang, A. Zheng, and X. Yang, Dynamic control of light propagation and optical switching through an RF-driven cascade-type atomic system, Phys. Lett. A **373**, 2992 (2009).
[53] Y.-Q. Li, S.-Z. Jin, and M. Xiao, Observation of an electromagnetically induced change of absorption in multilevel rubidium atoms, Phys. Rev. A **51**, R1754 (1995).
[54] A. J. Olson and S. K. Mayar, Electromagnetically induced transparency in rubidium, Am. J. Phys. **77**, 116 (2009).
[55] M. S. Safronova and U. I. Safronova, Critically evaluated theoretical energies, lifetimes, hyperfine constants, and multimode polarizabilities in ^{87}Rb, Phys. Rev. A **83**, 052508 (2011).